Developmental Cognitive Neuroscience 15 (2015) 117–129

Contents lists available at ScienceDirect

Developmental Cognitive Neuroscience

journal homepage: http://www.elsevier.com/locate/dcn

Dorsal anterior cingulate cortex in typically developing children: Laterality analysis

Jue Wang[a,b], Ning Yang[a,b,c], Wei Liao[d], Han Zhang[d], Chao-Gan Yan[a], Yu-Feng Zang[d], Xi-Nian Zuo[a,c,e,f,*]

[a] Key Laboratory of Behavioral Science and Magnetic Resonance Imaging Research Center, Institute of Psychology, Chinese Academy of Sciences, Beijing 100101, China
[b] University of Chinese Academy of Sciences, Beijing 100049, China
[c] Laboratory for Functional Connectome and Development, Institute of Psychology, Chinese Academy of Sciences, Beijing 100101, China
[d] Zhejiang Key Laboratory for Research in Assessment of Cognitive Impairments, Center for Cognition and Brain Disorders, Hangzhou Normal University, Hangzhou, Zhejiang 311121, China
[e] Faculty of Psychology, Southwest University, Chongqing 400715, China
[f] Department of Psychology, School of Education Science, Guangxi Teachers Education University, Guangxi 530001, China

ARTICLE INFO

Article history:
Received 27 February 2015
Received in revised form 3 October 2015
Accepted 5 October 2015
Available online 8 October 2015

Keywords:
Laterality
Anterior cingulate cortex
Cognitive control
Control network
Default mode
Development

ABSTRACT

We aimed to elucidate the dACC laterality in typically developing children and their sex/age-related differences with a sample of 84 right-handed children (6–16 years, 42 boys). We first replicated the previous finding observed in adults that gray matter density asymmetry in the dACC was region-specific: leftward (left > right) in its superior part, rightward (left < right) in its inferior part. Intrinsic connectivity analysis of these regions further revealed region-specific asymmetric connectivity profiles in dACC as well as their sex and age differences. Specifically, the superior dACC connectivity with frontoparietal network and the inferior dACC connectivity with visual network are rightward. The superior dACC connectivity with the default network (lateral temporal cortex) was more involved in the left hemisphere. In contrast, the inferior dACC connectivity with the default network (anterior medial prefrontal cortex) was more lateralized towards the right hemisphere. The superior dACC connectivity with lateral visual cortex was more distinct across two hemispheres in girls than that in boys. This connection in boys changed with age from right-prominent to left-prominent asymmetry whereas girls developed the connection from left-prominent to no asymmetry. These findings not only highlight the complexity and laterality of the dACC but also provided insights into dynamical structure–function relationships during the development.

1. Introduction

Based on its cytology, imaging characteristics and connections, the dorsal anterior cingulate cortex (dACC) is thought to play a crucial role in the development of human cognitive function and guiding human behaviors (Rushworth et al., 2007). It has been associated with cognitive control functions including attention modulation, competition monitoring, complex motor control, motivation, novelty, error detection, working memory, anticipation of cognitively demanding tasks, and the modulation of reward-based decision making (for review, see Shenhav et al., 2013). Functional abnormalities associated with the dACC have been consistently reported in ADHD (Bush et al., 1999; Cao et al., 2009; Castellanos et al., 2008; Durston, 2003; Rubia et al., 1999; Tamm et al., 2004; Tian et al., 2006; Yang et al., 2011; Zang et al., 2007), which is considered as a neurodevelopmental disorder (Bush et al., 2005; Castellanos et al., 2002).

Seldon has proposed that during human development, white matter grows outward and expands to the overlying cortex similar to a balloon, affecting the capacity of the cortex (Seldon, 2005). The different rates of expansion in particular brain regions create regional differences in cortical thickness, volume, surface area, neuronal density, curvature and folding patterns. A varying rate of expansion between homologous regions causes lateralization, which represents a natural feature of the human brain. Many

* Corresponding author at: Key Laboratory of Behavioral Science and Magnetic Resonance Imaging Research Center, Institute of Psychology, Chinese Academy of Sciences, Beijing 100101, China.
E-mail address: zuoxn@psych.ac.cn (X.-N. Zuo).
URL: http://lfcd.psych.ac.cn (X.-N. Zuo).

http://dx.doi.org/10.1016/j.dcn.2015.10.002

studies have reported the lateralization of the human brain, such as the leftward asymmetry of the precentral gyrus and the middle frontal, anterior temporal and superior parietal lobes, the rightward asymmetry of the inferior posterior temporal lobe and the inferior frontal gyrus (Luders et al., 2006) as well as larger right-than-left frontal petalias and larger left-than-right occipital petalias (Chiu and Damasio, 1980; LeMay, 1977). We recently demonstrated a specific pattern of gray matter density (GMD) asymmetry of the dACC in a large sample of healthy adults, indicating leftward GMD asymmetry in the superior dACC but rightward GMD asymmetry in the inferior dACC (Wang et al., 2013). Such an asymmetry has not been explored in typically developing children (TDC).

With increasing age, cortical thinning is observed in the occipital, parietal and somatosensory areas (Muftuler et al., 2011). This age-related GMD loss in TDC is explained by cortical maturation to increase functional efficiency and variety (Gogtay et al., 2004; Sowell et al., 2001, 2003, 2004). The dACC is typically considered to have strong reciprocal interconnections with the lateral prefrontal, parietal, and premotor and supplementary motor cortices (Bush et al., 2000). According to the evidence for age-related cortical thinning and the cortical expansion theory, we hypothesized that the GMD asymmetry in the dACC during childhood is associated with age.

Decreased lateralization of task activation in children and adolescents compared to adults has been detected for many tasks, including attention (Booth et al., 2003; Bunge et al., 2002; Moses et al., 2002) and language tasks (Holland et al., 2001; Szaflarski et al., 2006). The dACC connects with many brain networks involving language, attention and cognitive control, which are highly asymmetric in adults (Aboitiz et al., 1995; Corbetta and Shulman, 2002; Coull and Nobre, 1998; Garavan et al., 1999; Toga and Thompson, 2003). Increased functional connectivity between the left dACC and the left inferior frontal gyrus has been reported during a language-processing task, whereas increased connectivity between the right dACC and the right parietal areas during a visuo-spatial processing task was detectable (Stephan et al., 2003), suggesting that the brain regions associated with cognitive control in the dACC are restricted to the ipsilateral hemisphere. Computerized neurocognitive tests have provided strong evidence that substantial improvement with age occurred for executive functions, and relevant age–sex interactions (Gur et al., 2012). We thus further hypothesized that the morphologic asymmetry in the dACC would lead to its functional asymmetry with age and sex effects in TDC.

To directly test our hypotheses, we employed resting-state magnetic resonance imaging (rfMRI) as the method measuring intrinsic functional connectivity (iFC) (Biswal et al., 1995, 2010), which has been used to examine the ACC circuitry in human brains (Castellanos et al., 2008; Margulies et al., 2007; Tian et al., 2006; Yan et al., 2009). This tool has been proved valuable in studying neurodevelopment processes (Fair et al., 2007; Gao et al., 2013, 2014, 2015; Kelly et al., 2009; Betzel et al., 2014). With an approach similar to our previous study on asymmetric iFC pattern of the dACC in adults (Yan et al., 2009), we elucidate the dACC asymmetry profiles on both GMD and iFC in TDC as well as their interactions with age and sex.

2. Materials and methods

2.1. Participants

All participants are parts of a large longitudinal sample for the study of the normative growth curves of the brain in China, the Chinese Color Nest Program (CCNP). The CCNP data collection is currently undergoing, including three waves of multimodal neuroimaging data from 198 participants across five years (2012–2017). We have shared part of the CCNP wave-1 data to the public via the Consortium for Reliability and Reproducibility (CoRR) (Zuo and Xing, 2014; Zuo et al., 2014). Before the experiments, all participants or their guardians provided written informed consent. The Institutional Review Board of the Institute of Psychology of the Chinese Academy of Sciences approved the experiments. All participants had no history of head injury, psychiatric or neurological disorder or substance abuse according to their self-reports and their handedness was assessed using Annett's Inventory (Annett, 1976). We collected the wave-1 data from 162 participants at the time of manuscript preparation. A total of 42 participants were excluded from the samples based on the following criteria: (1) non-right-handed (13 participants); (2) poor anatomical image quality (2 participants); (3) bad spatial normalization based on visual inspection (4 participants); and (4) excessive head motion (23 participants). To match age and sex of samples, we finally selected 84 TDC from the 120 participants passing above criteria (6–16 years old, 42 males).

2.2. Data acquisition

All data were acquired using a 3T Siemens MR scanner (Magnetom Trio Tim equipped with syngo software) at Southwest University, Chongqing, China. To minimize head motion, foam pads and belts were used. T1-weighted image data were acquired using a magnetization prepared rapid gradient echo (MP-RAGE) sequence (176 sagittal slices, time repetition = 2600 ms, time echo = 3.02 ms, slice/gap thickness = 1/0 mm, in-plane matrix = 256×256, field of view = $256 \times 256\ mm^2$, and flip angle = 8°). Two rfMRI scans were acquired for each participant using a single-shot gradient-recalled echo planar imaging (EPI) sequence (repetition time = 2500 ms, echo time = 30 ms, flip angle = 80°, 38 axial slices, field of view = $216 \times 216\ mm^2$, in-plane matrix = 72×72, slice thickness = 3 mm, and slice overlapping = 10%) and were separated by the T1 scan. Each rfMRI scan contains 184 functional volumes in a total scan time of 460 s. The participants were instructed to rest with their eyes open and to look at a fixation point on the screen while not thinking of anything in particular or falling asleep. The rfMRI with smaller head motion measured by the mean frame-wise displacement (mean FD) as defined in (Power et al., 2012) was selected for subsequent analyses.

2.3. Overall strategy of laterality analysis

Similar to our previous studies (Wang et al., 2013; Yan et al., 2009), our analytic strategy consisted of eight fundamental stages: (1) creating a group-specific symmetric templates of gray matter, EPI image, and brain tissue mask for spatial normalization and iFC analyses; (2) preprocessing of the structural MRI and rfMRI scans; (3) generating individual GMD maps; (4) performing analysis of variance (ANOVA) with repeated measures to detect the differences in GMD between left and right sides of the brain, side-age, side-sex and side-sex-age interactions; (5) extracting peak coordinates for the dACC showing significant differences in left-right GMD asymmetry to define 3 mm-radius spheres as seed regions for subsequent iFC analysis; (6) generating individual iFC maps of the left and right dACC seeds; and (8) solving a similar ANOVA with repeated measures in (4) to determine the differences between the individual iFC maps of the left dACC seeds and the LR-flipped individual iFC maps of the right dACC seeds as well as their interactions with age and sex. The steps of image analysis are illustrated in Fig. 1, and the details of each of these steps are fully described in the subsequent sections.

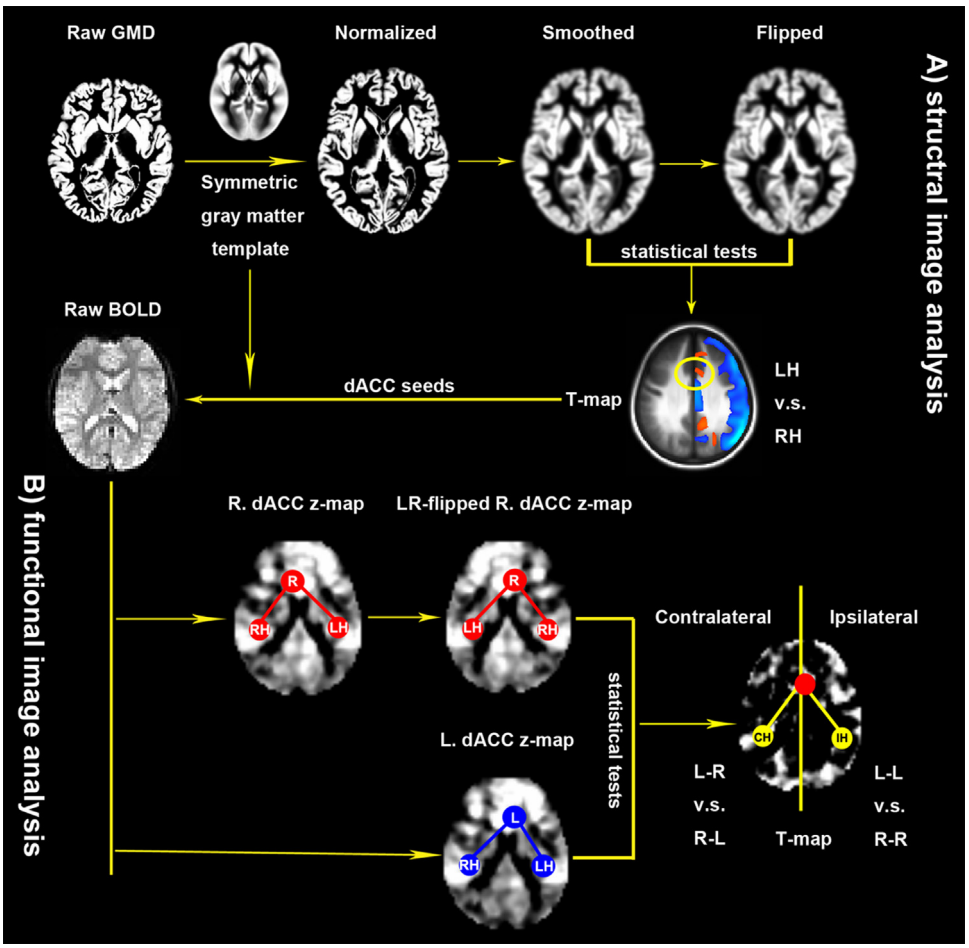

Fig. 1. Illustration of the overall procedure of image analysis. (A) Structural image analysis. Individual raw gray matter density (GMD) images are first normalized to a symmetric gray matter template in the standard brain space and then spatially smoothed. Paired *t*-tests were performed on smoothed GMD images and their left–right flipped (LR-flipped) versions to achieve a T-map for GMD differences between the left hemisphere (LH) and the right hemisphere (RH). This laterality map derives seeds of regions of interests for superior and inferior subdivisions of the dorsal cingulate cortex (dACC) for next steps of functional image analysis (B). In this second stage, individual raw BOLD images are first normalized to the symmetric standard brain template and then seed-based functional connectivity maps are estimated by using the dACC seeds in both hemispheres, and quantified with their Fisher's z-maps. Flexible factor analysis is employed to detect laterality effects on both ipsilateral (L-L versus R-R) and contralateral (L-R versus R-L) functional connectivity of the dACC using the left dACC (L.dACC) seeded z-maps and the LR-flipped versions (LR-flipped R.dACC) of the right dACC (R.dACC) seeded z-maps as inputs.

2.4. Creating symmetric templates and masks

Each individual GMD image was spatially normalized to the Montreal Neurological Institute (MNI) space and resampled with 1 mm isotropic voxel spatial resolution. To create a group-specific GMD template, we averaged all the normalized individual GMD images from the 84 TDC. This gray matter template was LR-flipped in the mid-sagittal plane ($x = 0$). The flipped and un-flipped gray matter templates were averaged to achieve a symmetric gray matter template for left–right spatial normalization (Luders et al., 2004). A symmetric EPI template was also created in the same manner. In addition, we created a symmetric brain mask for the calculation of the dACC iFC maps and the statistical correction for multiple comparisons. Specifically, we averaged and combined three brain tissues (i.e. gray matter, white matter and cerebrospinal fluid) and then binarized the combined brain tissue map. In the GMD analysis, only half of the brain symmetric mask was used to perform the correction for multiple comparisons regarding that the results in the two hemispheres are identical. We also created the symmetric masks for white matter and cerebral spinal fluid to extract the nuisance signal of covariates.

2.5. Structural MRI data analysis

Structural image preprocessing was carried out in the Data Processing Assistant for Resting-State fMRI (DPARSF) plugin (Version 2.2_121225) (Yan and Zang, 2010), which was developed based on the REST software toolbox (http://www.restfmri.net) (Song et al., 2011) and the Statistical Parametric Mapping toolbox (http://www.fil.ion.ucl.ac.uk/spm/software/spm8). Specifically, each structural image was first segmented into gray matter (GM), white matter (WM), and cerebrospinal fluid (CSF) using the tissue classification method termed unified segmentation in SPM8 (Ashburner and Friston, 2005). This step produced voxel-wise values representing the probability of a single voxel belonging to each of the three brain tissues. The individual GMD (unmodulated) images were subsequently spatially normalized to the symmetric gray matter template and then spatially smoothed using an isotropic Gaussian kernel of 12 mm full-width at half-maximum (FWHM). The individual smoothed GMD maps were then LR-flipped in the midsagittal plane ($x = 0$). Subsequent group analyses modeled the data with a flexible factorial ANOVA (repeated factor: side; non-repeated factor: sex; covariate of interests: age). Contrasts derived

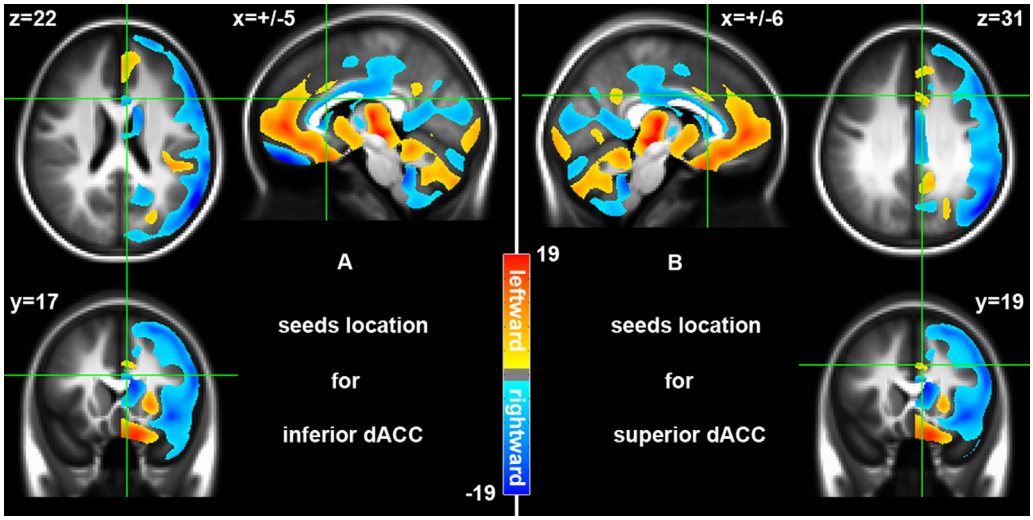

Fig. 2. Laterality of gray matter density (GMD) and its regional difference in dACC. T-maps of the paired *t*-tests on GMD between the left and the right hemisphere are overlaid onto the symmetric structural template. The warm colors indicate a leftward (left > right) laterality whereas the cool colors represents degree of a rightward (right > left) laterality of GMD. Region-specific asymmetry of GMD is detected in dACC where (A) inferior dACC seeds (±5, 17, 22) were rightward and (B) superior dACC seeds (±6, 19, 31) showed leftward asymmetry.

from this model can explicitly reveal side differences in GMD (i.e., asymmetry) and their interactions with age or sex (two-way interactions) as well as with age and sex (three-way interaction). To correct for multiple comparisons, we employed Gaussian Random Field (GRF)-based correction for controlling family wise error (FWE) constrained in the half brain symmetric mask (voxel-height threshold $p < 0.01$, corrected $p < 0.05$).

2.6. Functional MRI data preprocessing

The rfMRI image preprocessing, including disregarding the first 8 EPI volumes to allow for signal equilibration, slice timing correction, motion correction, nuisance covariates regression and spatial normalization, was also performed using the DPARSF plugin. Participants were excluded from the subsequent data analysis if their head motion exceeded 1.5 mm in translation or 1.5° in rotation in any direction. Various nuisance covariates including the WM and CSF mean time series and the motion time series from Friston 24-parameter head motion model (Yan et al., 2013a; Satterthwaite et al., 2013) were regressed out from the rfMRI images. Linear trends and unwanted components of time series outside 0.01–0.08 Hz were removed via linear de-trending and temporal filtering using the DPARSF plugin. The preprocessed individual rfMRI images were spatially normalized to the symmetric EPI template.

2.7. Seeds for functional connectivity analysis

As illustrated in Fig. 2, two clusters exhibited significant region-specific asymmetry of GMD within the dACC: rightward (right > left) asymmetry in the inferior part of the dACC (BA 24) (cold colors) and leftward (left > right) asymmetry in the superior part of the dACC (BA 32/24) (warm colors). For subsequent iFC asymmetry analyses of the dACC, we defined four seeds based on the two clusters. Specifically, the coordinates of the geometrical centers of these two clusters were manually extracted (the left inferior dACC: −5, 17, 22; the right inferior dACC: 5, 17, 22; the left superior dACC: −6, 19, 31; the left superior dACC: 6, 19, 31) in the MNI space. Four spheres with a radius of 3 mm (7 voxels, 189 mm^3) were created using each coordinate as a center.

2.8. Functional connectivity analysis

Using the REST toolkit, we performed seed-based iFC analyses using the four seeds of the dACC. For each participant, the representative time series was obtained by averaging the rfMRI time series of all voxels within the sphere for each of the four regions of interests. For each individual, four voxel-wise seed correlation maps were computed and then transformed to *z*-value maps using Fishers z-transformation (Lowe et al., 1998). The produced iFC maps were spatially smoothed using an 8 mm FWHM Gaussian kernel for subsequent statistical tests on iFC asymmetry of the dACC.

2.9. Statistical analysis of the iFC maps

For the examination of hemispheric iFC asymmetry, the processing method was the same as that of our previous study (Yan et al., 2009), which referenced two previous studies (Gong et al., 2005a; Huster et al., 2007). Specifically, we generated a new set of z-maps by LR-flipping the individual z-maps of the right hemispheric seeds (the right superior dACC and the right inferior dACC). For each seed, the un-flipped and flipped z-maps were then modeled by a flexible factorial ANOVA (repeated factor: side; non-repeated factor: sex; covariate of interests: age; nuisance covariates: global mean *z*-value and mean frame-wise displacement) similar as used in the GMD asymmetry analysis. Of note, the global mean *z* values were estimated for each individual and were then considered as a covariate in the model. This has been proved as an efficient standardization method for iFC analyses (Yan et al., 2013b). Design contrasts for this model can detect side differences in iFC (i.e., asymmetry or laterality) and their interactions with age or sex (two-way interactions) as well as with age and sex (three-way interaction). To correct for multiple comparisons, we applied GRF-based FWE correction within the EPI brain symmetric mask (voxel-height threshold $p < 0.01$, corrected $p < 0.05/2$). The corrected *p*-value was Bonferroni corrected according to the two regions of the dACC.

3. Results

The statistical analyses carried out in the present work generated a large number of results. Here we reported the main findings,

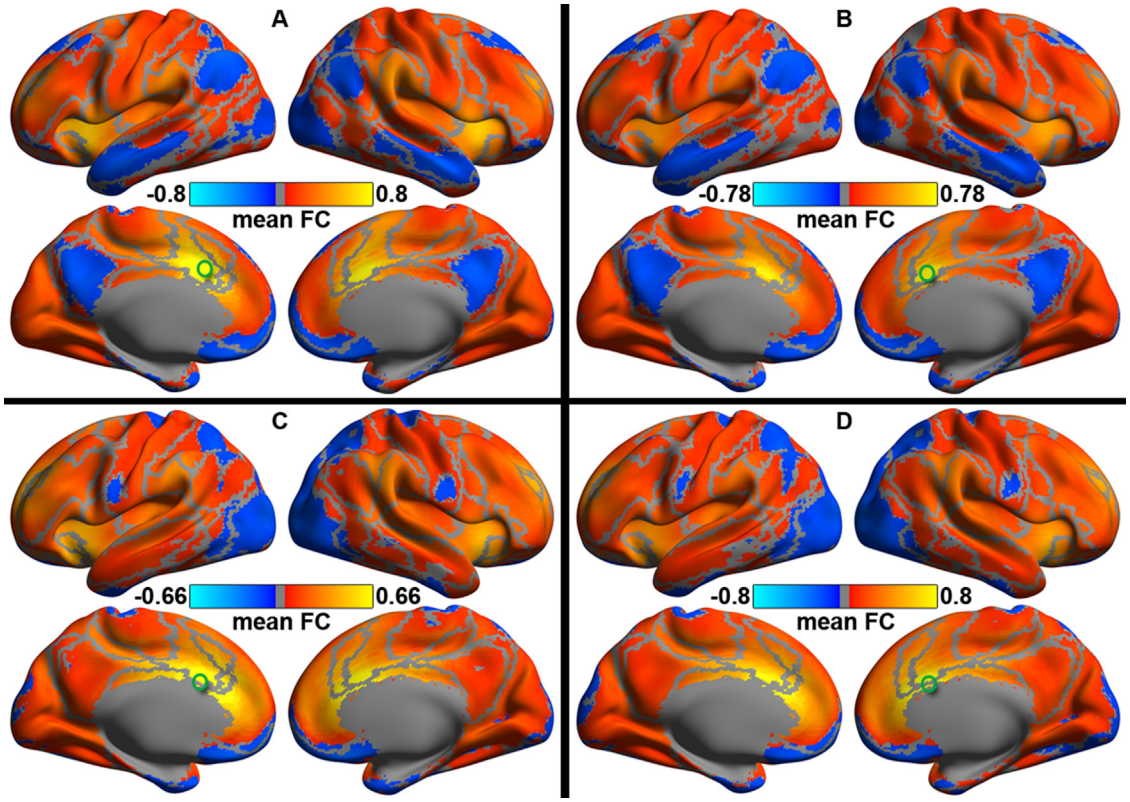

Fig. 3. Intrinsic functional connectivity (iFC) of the dorsal anterior cingulate cortex (dACC). Mean Fisher-z maps of all individual iFC of the four seeds for the superior (A: left hemisphere; B: right hemisphere) and inferior (C: left hemisphere; D: right hemisphere) dACC are rendered onto the Conte69_32k surfaces. All the maps displayed for lateral and medial views of both hemispheres. Gray curves indicate the boundaries between the seven networks in Yeo et al. (2011). The locations of the dACC seeds are labeled as a green circle on the surfaces.

and included some other results as in the supplementary text (e.g., age- and sex-related differences in GMD across the whole brain voxel-wise). The visualization module of the Connectome Computation System (http://github.com/zuoxinian/CCS) (Xu et al., 2015) was used to produce all figures presented in following sections.

3.1. Grey matter laterality in the dACC

As demonstrated in Fig. 2, in a typically developing sample, we replicated our previous findings observed in adults (Wang et al., 2013) by showing a clear region-specific asymmetry pattern in the dACC. This full brain GMD asymmetry analysis using the flexible factorial ANOVA indicated significant right > left (rightward) asymmetry in the inferior part of the dACC (BA24: Fig. 2A) but significant left > right (leftward) asymmetry in the superior part of the dACC (BA 32/24: Fig. 2B). No interaction effects on GMD asymmetry with age or sex were detectable for the dACC area (see supplementary Table S1 for regions showing interaction effects with age and sex).

3.2. Connectivity laterality in the dACC: main effects on side

Fig. 3 highlights both hemispheric commonalities and differences in the prominence of the dACC connectivity. The overall spatial patterns of iFC (group-level mean z maps) were highly similar across the left and right dACC seed regions (left superior versus right superior: Fig. 3A and B; left inferior versus right inferior: Fig. 3C and D). Consistent with previous studies (Kelly et al., 2009; Margulies et al., 2007; Yan et al., 2009), the superior dACC regions connected to a set of regions within the ventral attention network (Yeo et al., 2011) whereas inferior dACC regions connected to a set of areas within the fronto-parietal network. These two networks serve as two important parts of the brain control system (Cole et al., 2014b).

In our methods, the asymmetry of intra-hemispheric iFC of the dACC indicates the differences in dACC iFC with the ipsilateral hemisphere between left and right sides (i.e., LL versus RR). In contrast, the asymmetry of inter-hemispheric iFC of the dACC indicates differences in dACC iFC with the contralateral hemisphere between left and right sides (i.e., LR versus RL). The flexible factorial ANOVA did not find any side effects and their interactions with age and sex for global mean iFC of both superior and inferior parts of the dACC; however, this statistical model detected regionally specific side effects for both intra- and inter-hemispheric iFC of the dACC. All brain regions showing significant side effects on iFC with the two parts of the dACC were summarized in Table 1.

As shown in Fig. 4A, the superior dACC exhibited significantly higher RR iFC than LL iFC with multiple association cortical areas including the lateral temporal cortex (LTC), dorsal lateral prefrontal cortex (DLPFC), lateral parietal cortex (LPC), pre-supplementary motor area (preSMA) and dorsal medial prefrontal cortex (dMPFC). In contrast to the ipsilateral connectivity of the superior dACC, its contralateral connectivity with these areas showed inverse direction of the changes of individual differences (Fig. 4C). In addition, the superior dACC demonstrated distinct contralateral connectivity with the ventral posterior cingulate cortex (vPCC: LR > RL) and DLPFC/lateral occipital cortex (LOC) (LR < RL). The inferior dACC showed LL > RR connectivity with several clusters in LOC but RR > LL connectivity with anterior MPFC (aMPFC) (Fig. 5A). In Fig. 5C, the side effect on contralateral connectivity of the inferior dACC was depicted, indicating a different profile of hemispheric connectivity changes between DLPFC (LR > RL) and multiple MPFC clusters (LR < RL).

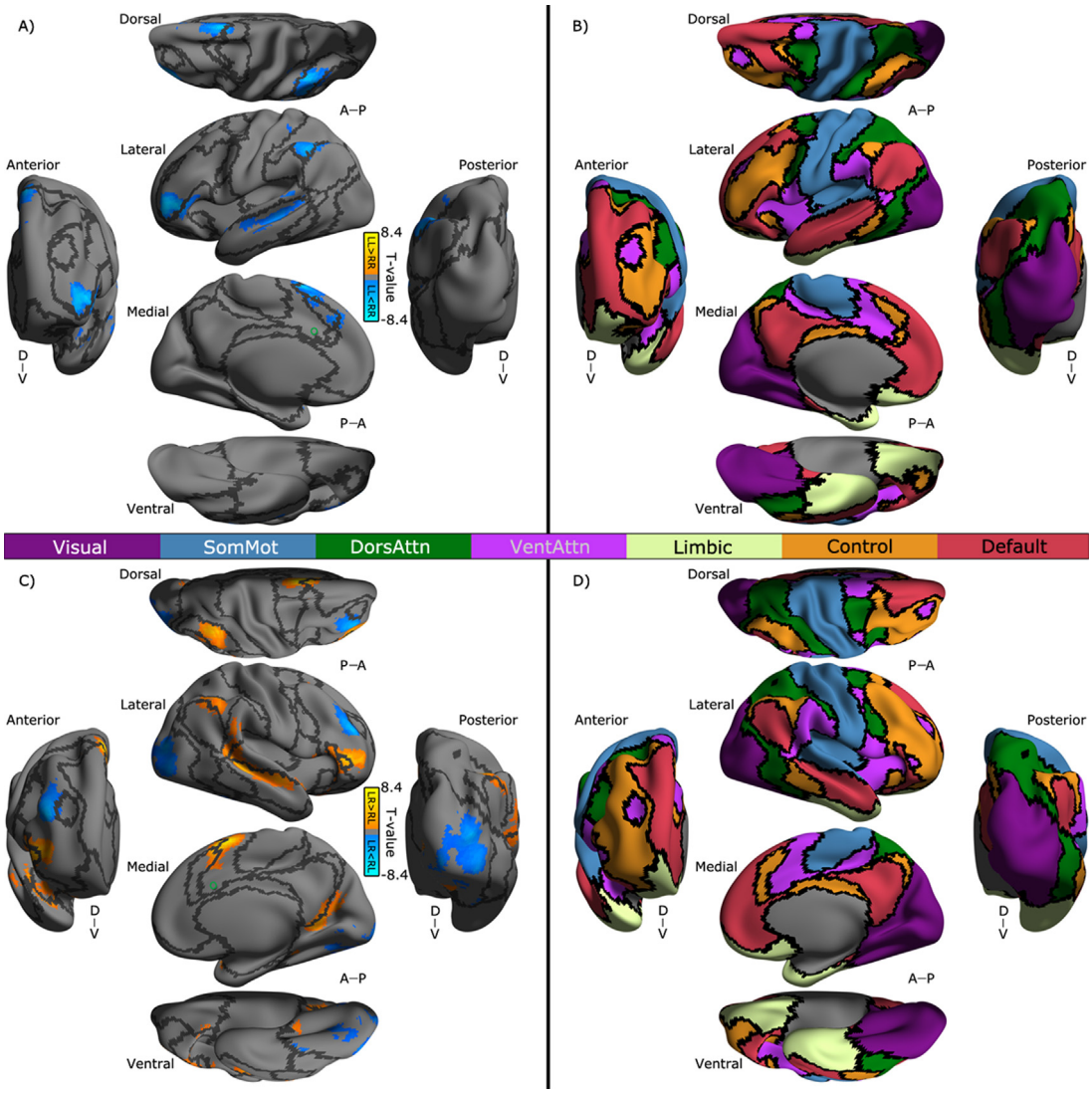

Fig. 4. Laterality of superior dACC's functional connectivity and its network distribution. *T*-value maps of the flexible factor analysis (see in Section 2) are rendered onto the Conte69_32k surfaces. Maps of the seven networks including visual (Visual), somatomotor (SomMot), dorsal attention (DorsAttn), ventral attention (VentAttn), limbic (Limbic), frontoparietal (Control) and default (Default) networks are also displayed on these surfaces. All the maps displayed for multiple views of both the ipsilateral hemisphere (A, B) and the contralateral hemisphere (C, D) in Conte69_32k space: A, anterior; P, posterior; D, dorsal; V, ventral. The functional network organization of the human cerebral cortex is derived from Yeo et al. (2011). Colors reflect regions estimated to be within the same network. Black curves indicate the boundaries between the networks. The locations of the superior dACC seeds are labeled as a green circle on the surfaces for laterality of (A) the ipsilateral functional connectivity (LL versus RR: warm colors for LL > RR, cool colors for LL < RR) and the contralateral functional connectivity (LR versus RL: warm colors for LR > RL, cool colors for LR < RL).

3.3. Connectivity laterality in the dACC: interaction with sex

The flexible factorial ANOVA detected an interaction between side and sex, indicating the differences in asymmetry profile of the dACC iFC between females and males. Only the superior dACC exhibited the side-sex interaction on its ipsilateral connectivity with the middle LOC (Fig. 6A). Fig. 6B further visualized this two-way interaction as scatter plots in details, and indicated a stronger LL > RR asymmetry of the dACC iFC with the middle LOC in females than that in males. See detailed description of the area in Table 2.

3.4. Connectivity laterality in the dACC: interaction with sex and age

With the ANOVA statistical tests, three-way interactions between side, sex and age were also detectable for ipsilateral connectivity of the superior dACC (Fig. 7A) and contralateral connectivity of the inferior dACC (Fig. 7C). Such interactions revealed differences in age-related changes of the dACC asymmetry profiles between females and males. Specifically, regarding the ipsilateral iFC between the superior dACC and the middle LOC, males exhibited a right-prominent (RR > LL) to left-prominent (LL > RR) asymmetry profile of the iFC along with age ($r = 0.60$, $p < 0.0001$) whereas females showed an inverse direction of asymmetry-age correlation ($r = -0.37$, $p = 0.0167$). In contrast, the contralateral iFC between the inferior dACC and the ventral medial occipital cortex (vMOC) demonstrated a positive correlation between its asymmetry profile (LR − RL) and age in females ($r = 0.57$, $p < 0.0001$) but a negative correlation in males ($r = -0.64$, $p < 0.0001$). Detailed description of these area were provided in Table 2.

4. Discussion

Using a typically developing sample (6–16 years old, 42 boys and 42 girls), we replicated a region-specific asymmetry pattern of gray matter density (GMD) within the dorsal anterior cingulate cortex (dACC), which was previously observed in adults (Wang et al., 2013): the distinction of morphology asymmetry

Table 1
Brain regions showing significant hemispheric asymmetry of intrinsic functional connectivity (iFC) with the dorsal anterior cingulate cortex (dACC).

Brain region	BA	MNI (*X Y Z*)			Peak *T* value	Cluster size (mm^3)	Mean peak iFC (SD)	
							Left dACC	Right dACC
i. Asymmetric connectivity with ipsilateral cerebral hemisphere LL > RR in the Superior dACC								
Cerebellum crus1		−42	−60	−30	4.76	15552	0.1218 (0.24)	−0.0008 (0.22)
ii. Asymmetric connectivity with ipsilateral cerebral hemisphere LL > RR in the Inferior dACC								
Middle occipital gyrus		−18	−78	21	4.27	14013	0.0262 (0.15)	−0.0362 (0.16)
iii. Asymmetric connectivity with ipsilateral cerebral hemisphere LL < RR in the Superior dACC								
Middle temporal lobe	21	−42	−36	0	−6.00	9261	-0.0938 (0.22)	0.0634 (0.22)
Inferior frontal gyrus	46	−48	48	6	−7.99	16443	0.0220 (0.20)	0.2632 (0.26)
Inferior parietal gyrus	40	−42	−48	39	−6.55	16416	0.0073 (0.22)	0.1422 (0.21)
iv. Asymmetric Connectivity with Ipsilateral Cerebral Hemisphere LL < RR in the Inferior dACC								
Anterior cingulate gyrus	32	−3	42	6	−5.65	10665	0.3512 (0.26)	0.4479 (0.24)
v. Asymmetric connectivity with contralateral cerebral hemisphere LR > RL in the Superior dACC								
Middle temporal gyrus	21	39	−36	0	6.97	47466	-0.0811 (0.19)	−0.2418 (0.18)
Middle frontal gyrus	46	48	48	6	7.32	13932	0.2090 (0.25)	0.0154 (0.19)
Supplementary motor area	6	6	12	63	8.33	1872	0.5062 (0.25)	0.2546 (0.20)
vi. Asymmetric connectivity with contralateral cerebral hemisphere LR > RL in the Inferior dACC								
Middle frontal gyrus	46	54	51	6	5.07	11691	0.0389 (0.19)	−0.0819 (0.20)
vii. Asymmetric connectivity with contralateral cerebral hemisphere LR < RL in the Superior dACC								
Cerebellum posterior lobe		27	−63	−27	−6.00	58239	0.0574 (0.19)	0.1726 (0.19)
Middle frontal gyrus	45	48	42	27	−6.17	10584	0.1056 (0.26)	0.2615 (0.26)

Table 2
Brain Regions showing significant gender/age interaction effect on intrinsic functional connectivity (iFC) with dorsal anterior cingulate cortex (dACC).

Brain region	BA	MNI (*X Y Z*)			Peak *T* value	Cluster size (mm^3)	Mean peak iFC (SD)	
							Left dACC	Right dACC
i. Side*Gender interaction of iFC with ipsilateral cerebral hemisphere in the superior dACC								
Middle occipital gyrus	19	−45	−93	12	4.14	7344	−0.0272 (0.19)	−0.0448 (0.18)
ii. Side*Gender*Age interaction of iFC with ipsilateral cerebral hemisphere in the superior dACC								
Middle occipital gyrus	19	−36	−93	12	−4.00	7533	−0.0298 (0.20)	−0.0842 (0.18)
iii. Side*Gender*Age interaction of iFC with contralateral cerebral hemisphere in the inferior dACC								
Cerebellum 4 5	37	27	−39	−27	4.80	7371	0.0652 (0.19)	0.0702 (0.16)

profiles of dACCs GMD (i.e., the rightward asymmetry of the inferior subdivision versus the leftward asymmetry of the superior subdivision). We further examined asymmetry changes of intrinsic functional connectivity (iFC) across the whole brain voxel-wise using regions derived from the morphologic asymmetry as seeds. This novel analysis revealed distinct asymmetry patterns between the two portions of dACC regarding their iFC profiles. Specifically, the superior dACC seed demonstrated leftward (LL > RR) asymmetry of connectivity with default network whereas the inferior dACC seed showed rightward (RR > LL) asymmetry of connectivity with default network. In addition, both the superior and the inferior dACC seeds exhibited rightward iFC asymmetry profiles with different networks (frontoparietal network versus visual network). Beyond the ipsilateral iFC asymmetry mentioned above, their contralateral iFC asymmetry was also detectable. Novel observations that how age and sex interact with these asymmetry iFC profiles were achieved in this developing sample. Regarding the fact that dACC belongs to multiple functional networks serving as a core region of the control system in the human brain (Margulies et al., 2007; Cole et al., 2014b,a), we discuss implications of these findings for understanding neural mechanism underlying brain asymmetry and their neurodevelopmental relevance from a network perspective (Yeo et al., 2011).

4.1. Children show region-specific laterality of dACC structure

Many previous studies have reported structural asymmetry of ACC, indicating that the right ACC had larger grey matter volume than in the left ACC (Huster et al., 2007; Paus et al., 1996) whereas the left anterior cingulum bundle (aCB) showed higher fractional anisotropy than that of the right aCB (O'Donnell et al., 2009; Takei et al., 2009; Huster et al., 2009; Gong et al., 2005a,b; Park et al., 2004; Fujiwara et al., 2007; Kubicki et al., 2003; Wang et al., 2013). Such asymmetry has been reported with high regional heterogeneity across the ACC in adults, especially for its dorsal part or cognitive subdivision (Wang et al., 2013). That is, the dACC presented rightward (right > left) asymmetry of GMD in its inferior portion whereas leftward (left > right) asymmetry in its superior portion. Our findings confirmed this region-specific asymmetry in typically developing children (6–16 years old), indicating the early presence of regional differences in morphological asymmetry within the dACC during the neurodevelopment. Such a complex profile of the dACC asymmetry might be an indication of the highly differentiated functions in both children and adults (Margulies et al., 2007; Kelly et al., 2009).

4.2. Dorsal ACC exhibits region-specific laterality of connectivity

The superior dACC seed belongs to the ventral attention network (Fig. 4) and exhibits significant iFC asymmetry with a set of areas across frontoparietal control network (Fig. 3A and B) and default network (Fig. 3A and B). These regions, dorsal lateral prefrontal cortex (DLPFC), anterior cingulate cortex (ACC) and lateral parietal cortex (LPC) within the frontoparietal network as well as dorsal medial prefrontal cortex (dMPFC) and lateral temporal cortex (LTC) within the default network, largely overlap with those

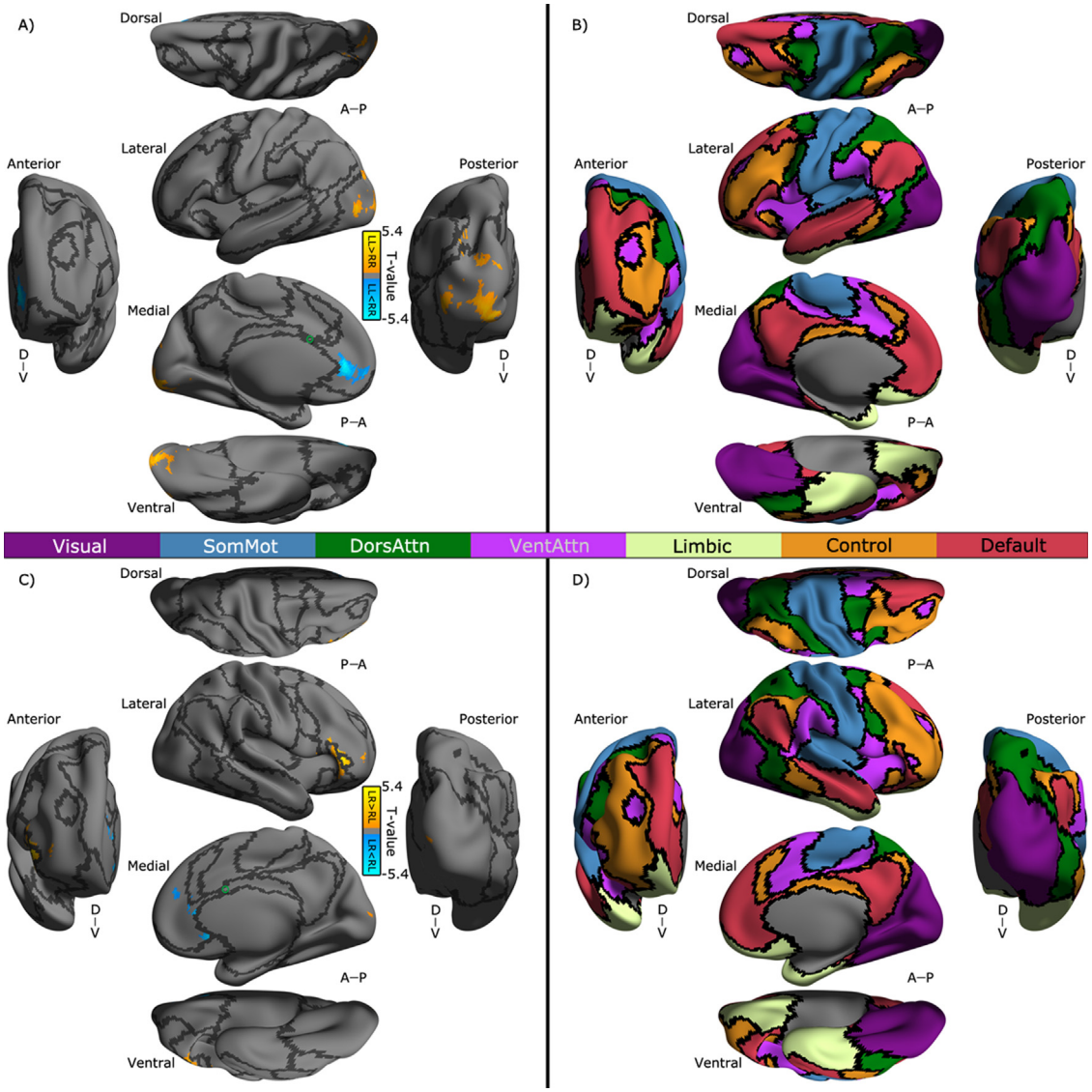

Fig. 5. Laterality of inferior dACC's functional connectivity and its network distribution. *T*-value maps of the flexible factor analysis (see in Section 2) are rendered onto the Conte69_32k surfaces. Maps of the seven networks including visual (Visual), somatomotor (SomMot), dorsal attention (DorsAttn), ventral attention (VentAttn), limbic (Limbic), frontoparietal (Control) and default (Default) networks are also displayed on these surfaces. All the maps displayed for multiple views of both the ipsilateral hemisphere (A, B) and the contralateral hemisphere (C, D) in Conte69_32k space: A, anterior; P, posterior; D, dorsal; V, ventral. The functional network organization of the human cerebral cortex is derived from Yeo et al. (2011). Colors reflect regions estimated to be within the same network. Black curves indicate the boundaries between the networks. The locations of the inferior dACC seeds are labeled as a green circle on the surfaces for laterality of (A) the ipsilateral functional connectivity (LL versus RR: warm colors for LL > RR, cool colors for LL < RR) and the contralateral functional connectivity (LR versus RL: warm colors for LR > RL, cool colors for LR < RL).

observed in our previous study of the iFC connectivity asymmetry of the cognitive subdivision in dACC (Yan et al., 2009). As discussed in the previous work, we speculate that these rightward asymmetry profiles on the strength of the dACCs iFC with DLPFC, ACC/dMPFC and LPC imply that relevant cognitive functions such as conflict-monitoring and spatial attention are right hemisphere based in children. In contrast, the dACC's iFC strength with LTC were stronger in the left hemisphere than that in the right hemisphere, suggesting related inhibition processes during decision-making, auditory and memory more involved in the left hemisphere. Beyond such a region-based explanation, using a well-established network parcellation (Yeo et al., 2011), we attempt to offer a systematic perspective on the connectivity asymmetry as following.

The frontoparietal control network serves as the flexible hub network to implement information initialization and exchange with other brain networks (Cole et al., 2014c) whereas the ventral attention network provides stable maintenance of different task sets (Dosenbach et al., 2006). The ventral attention network has been also termed as a salience network with a role of stimulus-driven attention control process, showing sustained and error-related activity (Seeley et al., 2007; Power and Petersen, 2013). Interactions between the salience network and the default network are crucial for implementing cognitive control (Fransson, 2005; Kelly et al., 2008; Sridharan et al., 2008; Menon and Uddin, 2010; Bonnelle et al., 2012). Our results indicated that default network, more specifically, its dMPFC subsystem for introspection about mental states (Andrews-Hanna et al., 2010, 2014; Andrews-Hanna, 2012), exhibited both leftward (LTC) and rightward (dMPFC) patterns of iFC with the superior dACC whereas frontoparietal network only exhibited rightward pattern of iFC with the superior dACC. The dACC has been recently assigned a single underlying function with an integrative theory (Shenhav et al., 2013). That is, allocating cognitive control based upon an evaluation of the expected value of control by integrating various factors

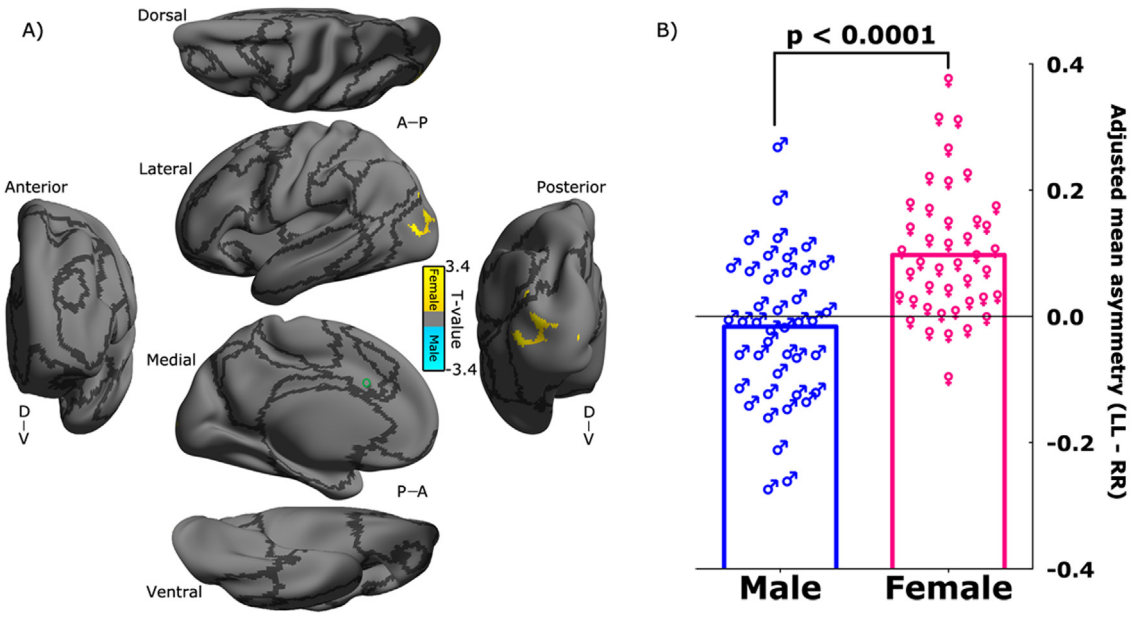

Fig. 6. Interaction between the laterality of superior dACC's ipsilateral functional connectivity and sex. (A) *T*-value maps of the flexible factor analysis (see in Section 2) are rendered onto the Conte69_32k surfaces. The maps displayed for multiple views of the ipsilateral hemisphere in Conte69_32k space: A, anterior; P, posterior; D, dorsal; V, ventral. Black curves indicate the boundaries between the seven neural networks. The location of the superior dACC seed is labeled as a green circle on the surfaces for laterality of the ipsilateral functional connectivity. The colorbar indicates different directions of the interaction: warm colors for female and cool colors for male. (B) Scatter bar plots are displayed for an intuitive illustration on the laterality–sex interaction in the region cluster as shown in (A). The laterality index is quantified with LL-RR adjusted for head motion and global mean connectivity.

of exchange between internal and external information to determine an optimal solution of control. The present work provided evidence that this control process may optimize its efficiency by distributing functional integration and functional inhibition into two hemispheres via the control and default networks (Raichle, 2015), respectively.

It is very interesting that the inferior part of the dACC, which belongs to the frontoparietal network, demonstrated a distinct pattern of iFC asymmetry compared to the superior part of the dACC (Fig. 4). Two regions, the anterior medial prefrontal cortex (aMPFC) as a core node of the default network (Fig. 3C and D), and lateral occipital cortex (LOC) of the visual network (Fig. 3C and D), both had stronger iFC (strength) with the dACC in the right hemisphere than that in the left hemisphere. Such a rightward functional asymmetry is in line with the morphological asymmetry of the inferior part of the dACC (Fig. 2), suggesting that the initiating and adjusting control of tasks implemented by the dACC connectivity with both default network and visual network are more based upon the right hemisphere (Yaakoby-Rotem and Geva, 2014). These findings not only provided evidence for the presence of the region-specific functional asymmetry within the dACC (i.e., superior versus inferior parts) in children but also supported highly heterogeneous functional interactions between dACC-anchored network and other brain networks according to their asymmetry profiles.

4.3. Laterality of dACC connectivity are sex- and age-dependent

Many studies have demonstrated sex differences in asymmetry of both structural and functional properties in the human brain (Toga and Thompson, 2003; Liu et al., 2009; Van Essen et al., 2012; Tomasi and Volkow, 2012; Nielsen et al., 2013). The effect of sex on structural properties related to the dACC has been examined by several studies (Hiscock et al., 1994; Zetzsche et al., 2001; Takao et al., 2011; Wang et al., 2013). A consistent finding is that males had higher fractional anisotropy in the aCB than females. Similar to Wang et al. (2013) but in children, no sex difference in GMD was observed in the dACC in the present work. Our work added novel findings to the existing literature by showing the detectable asymmetry of the ipsilateral iFC between the superior dACC seed and the LOC higher in females than that in males. Specifically, females had this connectivity more asymmetrically involved in the two hemispheres than males. This sex-specific connectivity asymmetry may be a reflection of the related morphological asymmetry in human visual cortex (Amunts et al., 2007), and might indicate that control-related components of implementing various visuospatial functions are more distinct between the two hemispheres in females that those in males (Smith, 2000; Hougaard et al., 2015).

Beyond our initial expectation, we observed no age-related changes in either morphology and iFC asymmetry in the dACC. It has been shown that age-related changes in hemispheric asymmetry depend on sex across the lifespan (Hausmann et al., 2003; Zuo et al., 2010). This indicates a potential three-way interaction among hemisphere, age and sex, which were detected with our statistical analyses of the dACC asymmetry in children (Fig. 6A and B). Boys had age-related changes of iFC between the superior dACC seed and LOC from right-prominent to left-prominent asymmetry. In contrast, girls iFC developed from left-prominent to no asymmetry. These findings revealed a sex-specific maturation pattern of the iFC asymmetry for the dACC and suggested distinct neurodevelopmental trajectories of functional connectivity underlying control-related asymmetry of the visuospatial processing between males and females (Chen et al., 2011).

4.4. Limitation and future direction

The voxel-wise method, which we developed previously (Yan et al., 2009), was extended to examine the asymmetry of the functional connectivity with dACC seed regions and its sex-related and age-related changes in typically developing children. This method revealed connectivity asymmetry for the dACC to both ipsilateral and contralateral hemispheres. Interpretation of the hemispheric

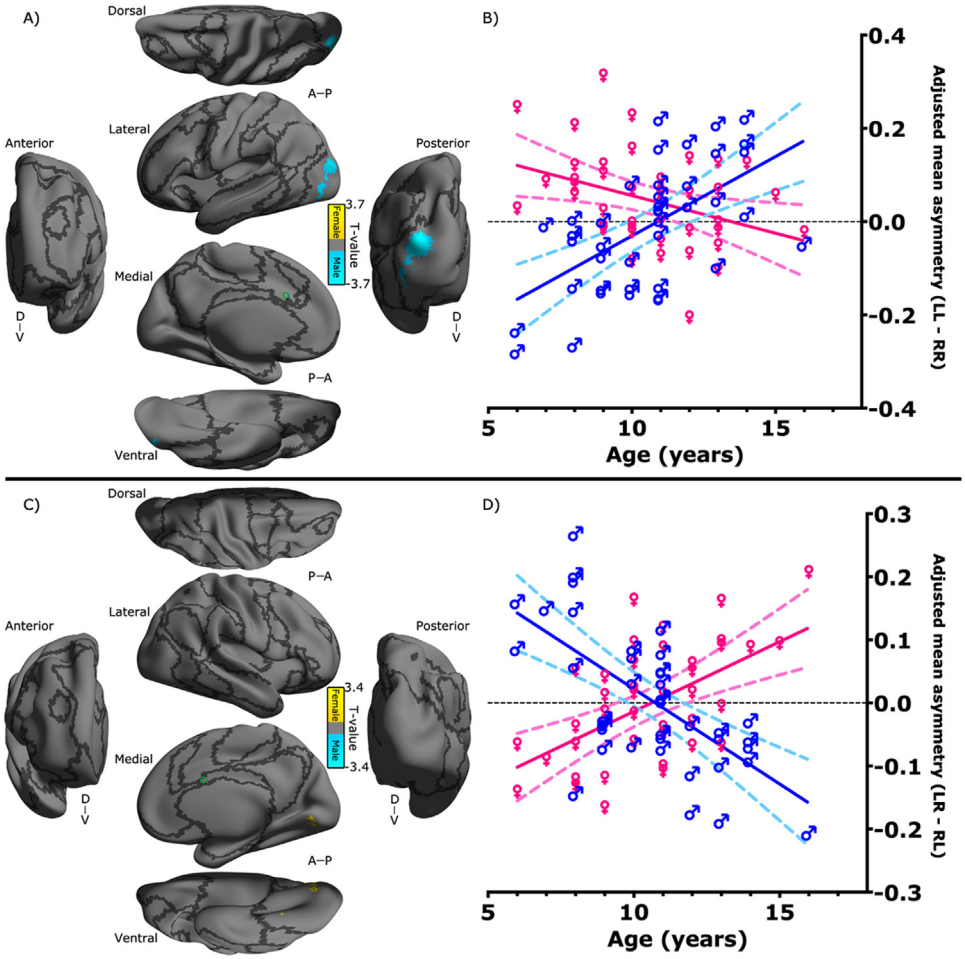

Fig. 7. Interactions among the laterality of dACC's functional connectivity, sex and age. *T*-value maps of the three-way interaction derived from the flexible factor analysis (see in Section 2) are rendered onto the Conte69_32k surfaces for (A) the superior dACC ipsilateral functional connectivity and (C) the inferior dACC contralateral functional connectivity. The maps displayed for multiple views of the ipsilateral hemisphere in Conte69_32k space: A, anterior; P, posterior; D, dorsal; V, ventral. Black curves indicate the boundaries between the seven neural networks. The locations of the superior and inferior dACC seeds are labeled as a green circle on the surfaces. The colorbar indicates different directions of the interaction. Scatter bar plots are displayed in (B) for an intuitive illustration on the three-way interaction in the region cluster as shown in (A), and in (D) for an intuitive illustration on the three-way interaction in the region cluster as shown in (C). The laterality index is quantified with LL-RR and LR-RL adjusted for head motion and global mean connectivity, respectively. Dashed curves indicate the 95% confidence intervals of the linear regression of the connectivity laterality on age.

asymmetry for ipsilateral connectivity (LL versus RR) was straightforward (left versus right) whereas the hemispheric asymmetry for contralateral connectivity was relatively complicated (LR versus RL) to interpret. Previous studies have combined the two types of asymmetry into a single lateral index (Liu et al., 2009) or reformed them into two lateral indices of hemispheric integration and segregation (Gotts et al., 2013). We did not define any lateral index explicitly but rather directly compared iFC maps with a flexible factor analysis model. Findings of both hemispheric asymmetry of the dACC connectivity were presented but only the ipsilateral connectivity asymmetry was discussed regarding its neurobiological and developmental significances. Our findings should be considered as preliminary regarding the use of cross-sectional data, particularly for the age-related 'changes' in the asymmetry of dACC connectivity. The ongoing CCNP project has a longitudinal study design, and will provide longitudinal data to further validate these findings.

We also note that the specificity of the current observations on the iFC laterality in terms of the seed locations derived from the morphological analyses in dACC. As emphasized in (Margulies et al., 2007; Kelly et al., 2009), the specific rostral/caudal location can make a notable difference in the functional connectivity. This highlights the sensitivity of seed-based iFC approaches to the location of seeds and its potential impacts on the lower test–retest reliability than other purely data-driven methods (Zuo and Xing, 2014). Our iFC analyses were informed by the gray matter laterality of the dACC and hopefully could improve both the reliability and validity. Such a strategy also provided a direct way of integrating both structure and function of the dACC regarding its laterality, leading an intuitive interpretation of the present findings. Comparisons of iFC laterality across different ways of selecting seeds and their influences on reliability and validity will be further investigated in future studies.

5. Conclusion

In summary, the present study provided further evidence that children exhibit similar region-specific asymmetry of dACC as in adults. Intrinsic connectivity analyses of this region-specific structural asymmetry further revealed region-specific dACC asymmetry regarding its functional connectivity with default, frontoparietal and visual networks. These functional asymmetric profiles are related to multiple factors such as sex and age in various cognitive control processes, indicating high functional complexity of the dACC.

Conflict of interest

All authors declared no conflict of interests.

Acknowledgements

We acknowledge the funding support from the National Basic Research Program (973 Program: 2015CB351702), the Natural Sciences Foundation of China (Major Fund for International Collaboration: 81220108014) and the Chinese Academy of Sciences Key Research Program (CAS: KSZD-EW-TZ-002). These funders had no role in study design, data collection or analysis, the decision to publish, or manuscript preparation. Dr. Zang acknowledges the support of the Qian Jiang Distinguished Professor Program. Dr. Zuo and Dr. Yan are members of the international collaboration team (under its trial stage with PI: Dr. Xun Liu) supported by the CAS K.C. Wong Education Foundation and acknowledge the support of the CAS Hundred Talents Program (XNZ: Y2CS112006; CGY: Y5CX072006). We thank the team led by Drs. Xu Chen, Jiang Qiu, Antao Chen in Southwest University for their endless support for data collection of the Chinese Color Nest Program and Dr. Richard Betzel from University of Pennsylvania for help with language editing and proof reading of the manuscript.

Appendix A. Supplementary data

Supplementary data associated with this article can be found, in the online version, at http://dx.doi.org/10.1016/j.dcn.2015.10.002.

References

Aboitiz, F., Ide, A., Navarrete, A., Pena, M., Rodriguez, E., Wolff, V., Zaidel, E., 1995. The anatomical substrates for language and hemispheric specialization. Biol. Res. 28, 45–50.

Amunts, K., Armstrong, E., Malikovic, A., Homke, L., Mohlberg, H., Schleicher, A., Zilles, K., 2007. Gender-specific left–right asymmetries in human visual cortex. J. Neurosci. 27, 1356–1364.

Andrews-Hanna, J.R., 2012. The brain's default network and its adaptive role in internal mentation. Neuroscientist 18, 251–270.

Andrews-Hanna, J.R., Reidler, J.S., Sepulcre, J., Poulin, R., Buckner, R.L., 2010. Functional-anatomic fractionation of the brain's default network. Neuron 65, 550–562.

Andrews-Hanna, J.R., Smallwood, J., Spreng, R.N., 2014. The default network and self-generated thought: component processes, dynamic control, and clinical relevance. Ann. N. Y. Acad. Sci. 1316, 29–52.

Annett, M., 1976. A coordination of hand preference and skill replicated. Br. J. Psychol. 67, 587–592.

Ashburner, J., Friston, K.J., 2005. Unified segmentation. Neuroimage 26, 839–851.

Betzel, R.F., Byrge, L., He, Y., Goni, J., Zuo, X.N., Sporns, O., 2014. Changes in structural and functional connectivity among resting-state networks across the human lifespan. Neuroimage 102 (Pt. 2), 345–357.

Biswal, B., Yetkin, F.Z., Haughton, V.M., Hyde, J.S., 1995. Functional connectivity in the motor cortex of resting human brain using echo-planar MRI. Magn. Reson. Med. 34, 537–541.

Biswal, B.B., Mennes, M., Zuo, X.N., Gohel, S., Kelly, C., Smith, S.M., Beckmann, C.F., Adelstein, J.S., Buckner, R.L., Colcombe, S., Dogonowski, A.M., Ernst, M., Fair, D., Hampson, M., Hoptman, M.J., Hyde, J.S., Kiviniemi, V.J., Kotter, R., Li, S.J., Lin, C.P., Lowe, M.J., Mackay, C., Madden, D.J., Madsen, K.H., Margulies, D.S., Mayberg, H.S., McMahon, K., Monk, C.S., Mostofsky, S.H., Nagel, B.J., Pekar, J.J., Peltier, S.J., Petersen, S.E., Riedl, V., Rombouts, S.A., Rypma, B., Schlaggar, B.L., Schmidt, S., Seidler, R.D., Siegle, G.J., Sorg, C., Teng, G.J., Veijola, J., Villringer, A., Walter, M., Wang, L., Weng, X.C., Whitfield-Gabrieli, S., Williamson, P., Windischberger, C., Zang, Y.F., Zhang, H.Y., Castellanos, F.X., Milham, M.P., 2010. Toward discovery science of human brain function. Proc. Natl. Acad. Sci. U. S. A. 107, 4734–4739.

Bonnelle, V., Ham, T.E., Leech, R., Kinnunen, K.M., Mehta, M.A., Greenwood, R.J., Sharp, D.J., 2012. Salience network integrity predicts default mode network function after traumatic brain injury. Proc. Natl. Acad. Sci. U. S. A. 109, 4690–4695.

Booth, J.R., Burman, D.D., Meyer, J.R., Lei, Z., Trommer, B.L., Davenport, N.D., Li, W., Parrish, T.B., Gitelman, D.R., Mesulam, M.M., 2003. Neural development of selective attention and response inhibition. Neuroimage 20, 737–751.

Bunge, S.A., Dudukovic, N.M., Thomason, M.E., Vaidya, C.J., Gabrieli, J.D., 2002. Immature frontal lobe contributions to cognitive control in children: evidence from fMRI. Neuron 33, 301–311.

Bush, G., Frazier, J.A., Rauch, S.L., Seidman, L.J., Whalen, P.J., Jenike, M.A., Rosen, B.R., Biederman, J., 1999. Anterior cingulate cortex dysfunction in attention-deficit/hyperactivity disorder revealed by fMRI and the counting stroop. Biol. Psychiatry 45, 1542–1552.

Bush, G., Luu, P., Posner, M.I., 2000. Cognitive and emotional influences in anterior cingulate cortex. Trends Cogn. Sci. 4, 215–222.

Bush, G., Valera, E.M., Seidman, L.J., 2005. Functional neuroimaging of attention-deficit/hyperactivity disorder: a review and suggested future directions. Biol. Psychiatry 57, 1273–1284.

Cao, X., Cao, Q., Long, X., Sun, L., Sui, M., Zhu, C., Zuo, X., Zang, Y., Wang, Y., 2009. Abnormal resting-state functional connectivity patterns of the putamen in medication-naive children with attention deficit hyperactivity disorder. Brain Res. 1303, 195–206.

Castellanos, F.X., Lee, P.P., Sharp, W., Jeffries, N.O., Greenstein, D.K., Clasen, L.S., Blumenthal, J.D., James, R.S., Ebens, C.L., Walter, J.M., Zijdenbos, A., Evans, A.C., Giedd, J.N., Rapoport, J.L., 2002. Developmental trajectories of brain volume abnormalities in children and adolescents with attention-deficit/hyperactivity disorder. J. Am. Med. Assoc. 288, 1740–1748.

Castellanos, F.X., Margulies, D.S., Kelly, C., Uddin, L.Q., Ghaffari, M., Kirsch, A., Shaw, D., Shehzad, Z., Di Martino, A., Biswal, B., Sonuga-Barke, E.J., Rotrosen, J., Adler, L.A., Milham, M.P., 2008. Cingulate-precuneus interactions: a new locus of dysfunction in adult attention-deficit/hyperactivity disorder. Biol. Psychiatry 63, 332–337.

Chen, P., Goedert, K.M., Murray, E., Kelly, K., Ahmeti, S., Barrett, A.M., 2011. Spatial bias and right hemisphere function: sex-specific changes with aging. J. Int. Neuropsychol. Soc. 17, 455–462.

Chiu, H.C., Damasio, A.R., 1980. Human cerebral asymmetries evaluated by computed tomography. J. Neurol. Neurosurg. Psychiatry 43, 873–878.

Cole, M.W., Bassett, D.S., Power, J.D., Braver, T.S., Petersen, S.E., 2014a. Intrinsic and task-evoked network architectures of the human brain. Neuron 83, 238–251.

Cole, M.W., Repovs, G., Anticevic, A., 2014b. The frontoparietal control system: a central role in mental health. Neuroscientist 20, 652–664.

Cole, M.W., Reynolds, J.R., Power, J.D., Repovs, G., Anticevic, A., Braver, T.S., 2014c. Multi-task connectivity reveals flexible hubs for adaptive task control. Nat. Neurosci. 16, 1348–1355.

Corbetta, M., Shulman, G.L., 2002. Control of goal-directed and stimulus-driven attention in the brain. Nat. Rev. Neurosci. 3, 201–215.

Coull, J.T., Nobre, A.C., 1998. Where and when to pay attention: the neural systems for directing attention to spatial locations and to time intervals as revealed by both PET and fMRI. J. Neurosci. 18, 7426–7435.

Dosenbach, N.U., Visscher, K.M., Palmer, E.D., Miezin, F.M., Wenger, K.K., Kang, H.C., Burgund, E.D., Grimes, A.L., Schlaggar, B.L., Petersen, S.E., 2006. A core system for the implementation of task sets. Neuron 50, 799–812.

Durston, S., 2003. A review of the biological bases of ADHD: what have we learned from imaging studies? Ment. Retard. Dev. Disabil. Res. Rev. 9, 184–195.

Fair, D.A., Dosenbach, N.U., Church, J.A., Cohen, A.L., Brahmbhatt, S., Miezin, F.M., Barch, D.M., Raichle, M.E., Petersen, S.E., Schlaggar, B.L., 2007. Development of distinct control networks through segregation and integration. Proc. Natl. Acad. Sci. U. S. A. 104, 13507–13512.

Fransson, P., 2005. Spontaneous low-frequency bold signal fluctuations: an fMRI investigation of the resting-state default mode of brain function hypothesis. Hum. Brain Mapp. 26, 15–29.

Fujiwara, H., Namiki, C., Hirao, K., Miyata, J., Shimizu, M., Fukuyama, H., Sawamoto, N., Hayashi, T., Murai, T., 2007. Anterior and posterior cingulum abnormalities and their association with psychopathology in schizophrenia: a diffusion tensor imaging study. Schizophr. Res. 95, 215–222.

Gao, W., Alcauter, S., Smith, J.K., Gilmore, J.H., Lin, W., 2015. Development of human brain cortical network architecture during infancy. Brain Struct. Funct. 220, 1173–1186.

Gao, W., Elton, A., Zhu, H., Alcauter, S., Smith, J.K., Gilmore, J.H., Lin, W., 2014. Intersubject variability of and genetic effects on the brain's functional connectivity during infancy. J. Neurosci. 34, 11288–11296.

Gao, W., Gilmore, J.H., Shen, D., Smith, J.K., Zhu, H., Lin, W., 2013. The synchronization within and interaction between the default and dorsal attention networks in early infancy. Cereb. Cortex 23, 594–603.

Garavan, H., Ross, T.J., Stein, E.A., 1999. Right hemispheric dominance of inhibitory control: an event-related functional MRI study. Proc. Natl. Acad. Sci. U. S. A. 96, 8301–8306.

Gogtay, N., Giedd, J.N., Lusk, L., Hayashi, K.M., Greenstein, D., Vaituzis, A.C., Nugent, T.F., Herman, D.H., Clasen, L.S., Toga, A.W., Rapoport, J.L., Thompson, P.M., 2004. Dynamic mapping of human cortical development during childhood through early adulthood. Proc. Natl. Acad. Sci. U. S. A. 101, 8174–8179.

Gong, G., Jiang, T., Zhu, C., Zang, Y., He, Y., Xie, S., Xiao, J., 2005a. Side and handedness effects on the cingulum from diffusion tensor imaging. Neuroreport 16, 1701–1705.

Gong, G., Jiang, T., Zhu, C., Zang, Y., Wang, F., Xie, S., Xiao, J., Guo, X., 2005b. Asymmetry analysis of cingulum based on scale-invariant parameterization by diffusion tensor imaging. Hum. Brain Mapp. 24, 92–98.

Gotts, S.J., Jo, H.J., Wallace, G.L., Saad, Z.S., Cox, R.W., Martin, A., 2013. Two distinct forms of functional lateralization in the human brain. Proc. Natl. Acad. Sci. U. S. A. 110, E3435–44.

Gur, R.C., Richard, J., Calkins, M.E., Chiavacci, R., Hansen, J.A., Bilker, W.B., Loughead, J., Connolly, J.J., Qiu, H., Mentch, F.D., Abou-Sleiman, P.M., Hakonarson, H., Gur, R.E., 2012. Age group and sex differences in performance on a computerized neurocognitive battery in children age 8–21. Neuropsychology 26, 251–265.

Hausmann, M., Gunturkun, O., Corballis, M., 2003. Age-related changes in hemispheric asymmetry depend on sex. Laterality 8, 277–290.
Hiscock, M., Inch, R., Jacek, C., Hiscock-Kalil, C., Kalil, K.M., 1994. Is there a sex difference in human laterality? I. An exhaustive survey of auditory laterality studies from six neuropsychology journals. J. Clin. Exp. Neuropsychol. 16, 423–435.
Holland, S.K., Plante, E., Weber Byars, A., Strawsburg, R.H., Schmithorst, V.J., Ball, W., 2001. Normal fMRI brain activation patterns in children performing a verb generation task. Neuroimage 14, 837–843.
Hougaard, A., Jensen, B.H., Amin, F.M., Rostrup, E., Hoffmann, M.B., Ashina, M., 2015. Cerebral asymmetry of fMRI-BOLD responses to visual stimulation. PLOS ONE 10, e0126477.
Huster, R.J., Westerhausen, R., Kreuder, F., Schweiger, E., Wittling, W., 2007. Morphologic asymmetry of the human anterior cingulate cortex. Neuroimage 34, 888–895.
Huster, R.J., Westerhausen, R., Kreuder, F., Schweiger, E., Wittling, W., 2009. Hemispheric and gender related differences in the midcingulum bundle: a DTI study. Hum. Brain Mapp. 30, 383–391.
Kelly, A.M., Uddin, L.Q., Biswal, B.B., Castellanos, F.X., Milham, M.P., 2008. Competition between functional brain networks mediates behavioral variability. Neuroimage 39, 527–537.
Kelly, C., de Zubicaray, G., Di Martino, A., Copland, D.A., Reiss, P.T., Klein, D.F., Castellanos, F.X., Milham, M.P., McMahon, K., 2009. L-dopa modulates functional connectivity in striatal cognitive and motor networks: a double-blind placebo-controlled study. J. Neurosci. 29, 7364–7378.
Kubicki, M., Westin, C.F., Nestor, P.G., Wible, C.G., Frumin, M., Maier, S.E., Kikinis, R., Jolesz, F.A., McCarley, R.W., Shenton, M.E., 2003. Cingulate fasciculus integrity disruption in schizophrenia: a magnetic resonance diffusion tensor imaging study. Biol. Psychiatry 54, 1171–1180.
LeMay, M., 1977. Asymmetries of the skull and handedness. phrenology revisited. J. Neurol. Sci. 32, 243–253.
Liu, H., Stufflebeam, S.M., Sepulcre, J., Hedden, T., Buckner, R.L., 2009. Evidence from intrinsic activity that asymmetry of the human brain is controlled by multiple factors. Proc. Natl. Acad. Sci. U. S. A. 106, 20499–20503.
Lowe, M.J., Mock, B.J., Sorenson, J.A., 1998. Functional connectivity in single and multislice echoplanar imaging using resting-state fluctuations. Neuroimage 7, 119–132.
Luders, E., Gaser, C., Jancke, L., Schlaug, G., 2004. A voxel-based approach to gray matter asymmetries. Neuroimage 22, 656–664.
Margulies, D.S., Kelly, A.M., Uddin, L.Q., Biswal, B.B., Castellanos, F.X., Milham, M.P., 2007. Mapping the functional connectivity of anterior cingulate cortex. Neuroimage 37, 579–588.
Menon, V., Uddin, L.Q., 2010. Saliency, switching, attention and control: a network model of insula function. Brain Struct. Funct. 214, 655–667.
Moses, P., Roe, K., Buxton, R.B., Wong, E.C., Frank, L.R., Stiles, J., 2002. Functional MRI of global and local processing in children. Neuroimage 16, 415–424.
Muftuler, L.T., Davis, E.P., Buss, C., Head, K., Hasso, A.N., Sandman, C.A., 2011. Cortical and subcortical changes in typically developing preadolescent children. Brain Res. 1399, 15–24.
Nielsen, J.A., Zielinski, B.A., Ferguson, M.A., Lainhart, J.E., Anderson, J.S., 2013. An evaluation of the left-brain vs. right-brain hypothesis with resting state functional connectivity magnetic resonance imaging. PLoS ONE 8, e71275.
O'Donnell, L.J., Westin, C.F., Golby, A.J., 2009. Tract-based morphometry for white matter group analysis. Neuroimage 45, 832–844.
Park, H.J., Westin, C.F., Kubicki, M., Maier, S.E., Niznikiewicz, M., Baer, A., Frumin, M., Kikinis, R., Jolesz, F.A., McCarley, R.W., Shenton, M.E., 2004. White matter hemisphere asymmetries in healthy subjects and in schizophrenia: a diffusion tensor MRI study. Neuroimage 23, 213–223.
Paus, T., Otaky, N., Caramanos, Z., MacDonald, D., Zijdenbos, A., D'Avirro, D., Gutmans, D., Holmes, C., Tomaiuolo, F., Evans, A.C., 1996. In vivo morphometry of the intrasulcal gray matter in the human cingulate, paracingulate, and superior-rostral sulci: hemispheric asymmetries, gender differences and probability maps. J. Comp. Neurol. 376, 664–673.
Power, J.D., Barnes, K.A., Snyder, A.Z., Schlaggar, B.L., Petersen, S.E., 2012. Spurious but systematic correlations in functional connectivity MRI networks arise from subject motion. Neuroimage 59, 2142–2154.
Power, J.D., Petersen, S.E., 2013. Control-related systems in the human brain. Curr. Opin. Neurobiol. 23, 223–228.
Raichle, M.E., 2015. The brain's default mode network. Annu. Rev. Neurosci. 38, 433–447.
Rubia, K., Overmeyer, S., Taylor, E., Brammer, M., Williams, S.C., Simmons, A., Bullmore, E.T., 1999. Hypofrontality in attention deficit hyperactivity disorder during higher-order motor control: a study with functional MRI. Am. J. Psychiatry 156, 891–896.
Rushworth, M.F., Buckley, M.J., Behrens, T.E., Walton, M.E., Bannerman, D.M., 2007. Functional organization of the medial frontal cortex. Curr. Opin. Neurobiol. 17, 220–227.
Satterthwaite, T.D., Wolf, D.H., Ruparel, K., Erus, G., Elliott, M.A., Eickhoff, S.B., Gennatas, E.D., Jackson, C., Prabhakaran, K., Smith, A., Hakonarson, H., Verma, R., Davatzikos, C., Gur, R.E., Gur, R.C., 2013. Heterogeneous impact of motion on fundamental patterns of developmental changes in functional connectivity during youth. Neuroimage 83, 45–57.
Seeley, W.W., Menon, V., Schatzberg, A.F., Keller, J., Glover, G.H., Kenna, H., Reiss, A.L., Greicius, M.D., 2007. Dissociable intrinsic connectivity networks for salience processing and executive control. J. Neurosci. 27, 2349–2356.
Seldon, H.L., 2005. Does brain white matter growth expand the cortex like a balloon? Hypothesis and consequences. Laterality 10, 81–95.
Shenhav, A., Botvinick, M.M., Cohen, J.D., 2013. The expected value of control: an integrative theory of anterior cingulate cortex function. Neuron 79, 217–240.
Smith, W.M., 2000. Hemispheric and facial asymmetry: gender differences. Laterality 5, 251–258.
Song, X.W., Dong, Z.Y., Long, X.Y., Li, S.F., Zuo, X.N., Zhu, C.Z., He, Y., Yan, C.G., Zang, Y.F., 2011. REST: a toolkit for resting-state functional magnetic resonance imaging data processing. PLoS ONE 6, e25031.
Sowell, E.R., Peterson, B.S., Thompson, P.M., Welcome, S.E., Henkenius, A.L., Toga, A.W., 2003. Mapping cortical change across the human life span. Nat. Neurosci. 6, 309–315.
Sowell, E.R., Thompson, P.M., Leonard, C.M., Welcome, S.E., Kan, E., Toga, A.W., 2004. Longitudinal mapping of cortical thickness and brain growth in normal children. J. Neurosci. 24, 8223–8231.
Sowell, E.R., Thompson, P.M., Tessner, K.D., Toga, A.W., 2001. Mapping continued brain growth and gray matter density reduction in dorsal frontal cortex: inverse relationships during postadolescent brain maturation. J. Neurosci. 21, 8819–8829.
Sridharan, D., Levitin, D.J., Menon, V., 2008. A critical role for the right fronto-insular cortex in switching between central-executive and default-mode networks. Proc. Natl. Acad. Sci. U. S. A. 105, 12569–12574.
Stephan, K.E., Marshall, J.C., Friston, K.J., Rowe, J.B., Ritzl, A., Zilles, K., Fink, G.R., 2003. Lateralized cognitive processes and lateralized task control in the human brain. Science 301, 384–386.
Szaflarski, J.P., Holland, S.K., Schmithorst, V.J., Byars, A.W., 2006. fMRI study of language lateralization in children and adults. Hum. Brain Mapp. 27, 202–212.
Takao, H., Hayashi, N., Ohtomo, K., 2011. White matter asymmetry in healthy individuals: a diffusion tensor imaging study using tract-based spatial statistics. Neuroscience 193, 291–299.
Takei, K., Yamasue, H., Abe, O., Yamada, H., Inoue, H., Suga, M., Muroi, M., Sasaki, H., Aoki, S., Kasai, K., 2009. Structural disruption of the dorsal cingulum bundle is associated with impaired stroop performance in patients with schizophrenia. Schizophr. Res. 114, 119–127.
Tamm, L., Menon, V., Ringel, J., Reiss, A.L., 2004. Event-related fMRI evidence of frontotemporal involvement in aberrant response inhibition and task switching in attention-deficit/hyperactivity disorder. J. Am. Acad. Child Adolesc. Psychiatry 43, 1430–1440.
Tian, L., Jiang, T., Wang, Y., Zang, Y., He, Y., Liang, M., Sui, M., Cao, Q., Hu, S., Peng, M., Zhuo, Y., 2006. Altered resting-state functional connectivity patterns of anterior cingulate cortex in adolescents with attention deficit hyperactivity disorder. Neurosci. Lett. 400, 39–43.
Toga, A.W., Thompson, P.M., 2003. Mapping brain asymmetry. Nat. Rev. Neurosci. 4, 37–48.
Tomasi, D., Volkow, N.D., 2012. Laterality patterns of brain functional connectivity: gender effects. Cereb. Cortex 22, 1455–1462.
Van Essen, D.C., Glasser, M.F., Dierker, D.L., Harwell, J., Coalson, T., 2012. Parcellations and hemispheric asymmetries of human cerebral cortex analyzed on surface-based atlases. Cereb. Cortex 22, 2241–2262.
Wang, J., Liu, D.Q., Zhang, H., Zhu, W.X., Dong, Z.Y., Zang, Y.F., 2013. Asymmetry of the dorsal anterior cingulate cortex: evidences from multiple modalities of MRI. Neuroinformatics 11, 149–157.
Xu, T., Yang, Z., Jang, L.L., Xing, X.X., Zuo, X.N., 2015. A connectome computation system for discovery science of brain. Sci. Bull. 60, 86–95.
Yaakoby-Rotem, S., Geva, R., 2014. Asymmetric attention networks: the case of children. J. Int. Neuropsychol. Soc. 20, 434–443.
Yan, C.G., Cheung, B., Kelly, C., Colcombe, S., Craddock, R.C., Di Martino, A., Li, Q., Zuo, X.N., Castellanos, F.X., Milham, M.P., 2013a. A comprehensive assessment of regional variation in the impact of head micromovements on functional connectomics. Neuroimage 76, 183–201.
Yan, C.G., Craddock, R.C., Zuo, X.N., Zang, Y.F., Milham, M.P., 2013b. Standardizing the intrinsic brain: towards robust measurement of inter-individual variation in 1000 functional connectomes. Neuroimage 80, 246–262.
Yan, C.G., Zang, Y., 2010. DPARSF: a MATLAB toolbox for "pipeline" data analysis of resting-state fMRI. Front. Syst. Neurosci. 4, 13.
Yan, H., Zuo, X.N., Wang, D., Wang, J., Zhu, C., Milham, M.P., Zhang, D., Zang, Y., 2009. Hemispheric asymmetry in cognitive division of anterior cingulate cortex: a resting-state functional connectivity study. Neuroimage 47, 1579–1589.
Yang, H., Wu, Q.Z., Guo, L.T., Li, Q.Q., Long, X.Y., Huang, X.Q., Chan, R.C., Gong, Q.Y., 2011. Abnormal spontaneous brain activity in medication-naive ADHD children: a resting state fMRI study. Neurosci. Lett. 502, 89–93.
Yeo, B.T., Krienen, F.M., Sepulcre, J., Sabuncu, M.R., Lashkari, D., Hollinshead, M., Roffman, J.L., Smoller, J.W., Zollei, L., Polimeni, J.R., Fischl, B., Liu, H., Buckner, R.L., 2011. The organization of the human cerebral cortex estimated by intrinsic functional connectivity. J. Neurophysiol. 106, 1125–1165.
Zang, Y.F., He, Y., Zhu, C.Z., Cao, Q.J., Sui, M.Q., Liang, M., Tian, L.X., Jiang, T.Z., Wang, Y.F., 2007. Altered baseline brain activity in children with ADHD revealed by resting-state functional MRI. Brain Dev. 29, 83–91.
Zetzsche, T., Meisenzahl, E.M., Preuss, U.W., Holder, J.J., Kathmann, N., Leinsinger, G., Hahn, K., Hegerl, U., Moller, H.J., 2001. In-vivo analysis of the human planum temporale (PT): does the definition of PT borders influence the results with regard to cerebral asymmetry and correlation with handedness? Psychiatry Res. 107, 99–115.
Zuo, X.N., Anderson, J.S., Bellec, P., Birn, R.M., Biswal, B.B., Blautzik, J., Breitner, J.C., Buckner, R.L., Calhoun, V.D., Castellanos, F.X., Chen, A., Chen, B., Chen, J., Chen,

X., Colcombe, S.J., Courtney, W., Craddock, R.C., Di Martino, A., Dong, H.M., Fu, X., Gong, Q., Gorgolewski, K.J., Han, Y., He, Y., He, Y., Ho, E., Holmes, A., Hou, X.H., Huckins, J., Jiang, T., Jiang, Y., Kelley, W., Kelly, C., King, M., LaConte, S.M., Lainhart, J.E., Lei, X., Li, H.J., Li, K., Li, K., Lin, Q., Liu, D., Liu, J., Liu, X., Liu, Y., Lu, G., Lu, J., Luna, B., Luo, J., Lurie, D., Mao, Y., Margulies, D.S., Mayer, A.R., Meindl, T., Meyerand, M.E., Nan, W., Nielsen, J.A., O'Connor, D., Paulsen, D., Prabhakaran, V., Qi, Z., Qiu, J., Shao, C., Shehzad, Z., Tang, W., Villringer, A., Wang, H., Wang, K., Wei, D., Wei, G.X., Weng, X.C., Wu, X., Xu, T., Yang, N., Yang, Z., Zang, Y.F., Zhang, L., Zhang, Q., Zhang, Z., Zhang, Z., Zhao, K., Zhen, Z., Zhou, Y., Zhu, X.T., Milham, M.P., 2014. An open science resource for establishing reliability and reproducibility in functional connectomics. Sci. Data 1, 140049.

Zuo, X.N., Kelly, C., Di Martino, A., Mennes, M., Margulies, D.S., Bangaru, S., Grzadzinski, R., Evans, A.C., Zang, Y.F., Castellanos, F.X., Milham, M.P., 2010. Growing together and growing apart: regional and sex differences in the lifespan developmental trajectories of functional homotopy. J. Neurosci. 30, 15034–15043.

Zuo, X.N., Xing, X.X., 2014. Test–retest reliabilities of resting-state FMRI measurements in human brain functional connectomics: a systems neuroscience perspective. Neurosci. Biobehav. Rev. 45, 100–118.